High Frequency LLC Resonant Converter with Magnetic Shunt Integrated Planar Transformer

Mingxiao Li, Ziwei Ouyang, Michael A. E. Andersen
Department of Electrical Engineering, Technical University of Denmark
Elektrovej, Building 325
2800 Kongens Lyngby, Denmark
lmxedward.jackman@gmail.com, zo@elektro.dtu.dk, ma@elektro.dtu.dk

***Abstract*—High Frequency LLC requires a smaller resonant inductance which is usually implemented by transformer leakage inductance. However, this small resonant inductance is difficult to deal with a wide input voltage range. This paper proposes a new method to implement a larger resonant inductance by using a magnetic shunt integrated into planar transformer. The switching frequency can be greatly narrowed by designing a smaller inductance ratio of magnetizing inductance to resonant inductance. Since this method can well deal with a wide input voltage range without adding extra inductor and increasing the size of the transformer, the power density can be improved. The precise leakage inductance calculation method for this transformer and detailed LLC converter design procedure are presented. A 280-380V and 48V-100W half bridge LLC resonant converter with 1 MHz resonant frequency is built to verify the design methodology.**

Keywords—magnetic shunt; LLC resonant converter; planar transformer; narrowed swithing frequency

I. INTRODUCTION

There has been a long desire for converter miniaturization to increase its power density and efficiency. LLC resonant converter has been proved as an excellent candidate to satisfy these requirements by increasing its operating frequency and integrating its magnetic components. It has become a popular converter and been used in many applications [1]-[4].

LLC can achieve the maximum efficiency at the resonant frequency. However, to maintain constant output under a wide input voltage range, LLC has to operate in a large frequency range. Usually, it is designed to operate below the resonant frequency. Many publications have analyzed the hold-up time compensation. The literature [5] proposes a structure to decrease the magnetizing inductance during the hold-up time so as to obtain the high voltage gain. However, the primary current increases with the decreased magnetizing inductance, large conduction loss, turn-off loss, additional winding and core loss due to the auxiliary winding are generated. The same issue also exists in literature [6] that proposes a new topology to increase peak gain by adding a capacitor in series with the magnetizing inductance. The equivalent magnetizing inductance decreases when switching frequency reduces to obtain a high voltage gain. Besides, none of them tests their methodology in high frequency-MHz operation.

An alternative to achieve high voltage gain with narrowed operating frequency range can be done by designing the large resonant inductor to create the low inductance ratio of magnetizing inductance to resonant inductance. However, the large inductor means the increase of the number of windings and additional magnetic core. Thus more winding and core loss is generated and the power density is reduced. Additionally, for LLC operating at high frequency, the resonant inductor is usually integrated into the planar transformer by utilizing its leakage inductance to increase its power density [7]. Interleaving structure is always implemented to reduce AC resistance by minimizing the leakage energy, causing the smaller leakage inductance and large inductance ratio. Thus the regulation capability is reduced.

One method to create large planar transformer leakage inductance by inserting a magnetic shunt is proposed in [8] and the relation between the leakage inductance and the characteristic of magnetic shunt is investigated in [9]. An accurate prediction of leakage inductance for the planar transformer is provided in [8]. It considers the energy in the primary side, secondary side and magnetic shunt and gives the equation to calculate the leakage inductance referred to the primary side of the planar transformer with a magnetic shunt. However, this is only valid when both primary and secondary windings are adjacent to the magnetic shunt, as shown in Fig.1. An air gap needs to be inserted to get the required magnetizing inductance, but the winding loss increases significantly because of the fringing effect brought by flux around air gap.

To maximize the leakage inductance without additional winding loss, a novel planar transformer structure with both primary and secondary windings located away from magnetic shunt is proposed. The energy stored in the window cannot be neglected to calculate the leakage inductance when both primary and secondary windings are located away from the magnetic shunt.

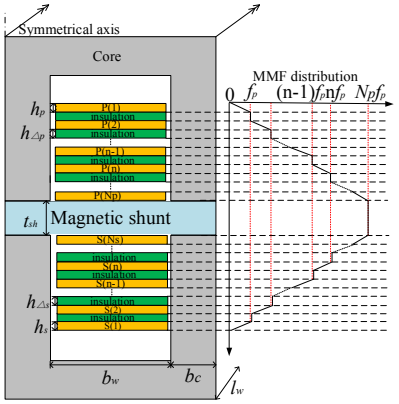

Fig.1. MMF distribution for the shunt-inserted planar transformer with both primary and secondary windings adjacent to the shunt[8]

This paper is organized as follows. Section II elaborates the analysis of the leakage inductance and proposes a formula to calculate the leakage inductance for the proposed transformer structure. Although the leakage inductance is decreased with increasing frequency [10], the deviation is significantly small and can be neglect. Section III gives the detailed design procedure for a high performance LLC converter. In section IV, a 1MHz 100W converter is built to demonstrate the proposed transformer structure. Section V concludes the paper.

II. Proposed Transformer Structure

The proposed transformer structure is shown in Fig.2. Both primary and secondary windings are located away from shunt with controllable distance. The air gap is inserted to get required magnetizing inductance, while has negligible effect on leakage inductance.

The leakage energy contains the energy in the primary and secondary windings, the air and the magnetic shunt. $f_p=k_pI_p$ is the magnetomotive force (MMF) in each layer of the primary windings. k_p is the number of turns on each layer of primary windings. N_p is the number of turns for primary side. The MMF in the window area can be assumed to be N_pf_p. Then the energy in the window area can be specified. Thus the leakage inductance is obtained by

$$E=\frac{1}{2}\int_V B\times HdV=\frac{1}{2}\cdot L_k\cdot I_p^{\,2} \tag{1}$$

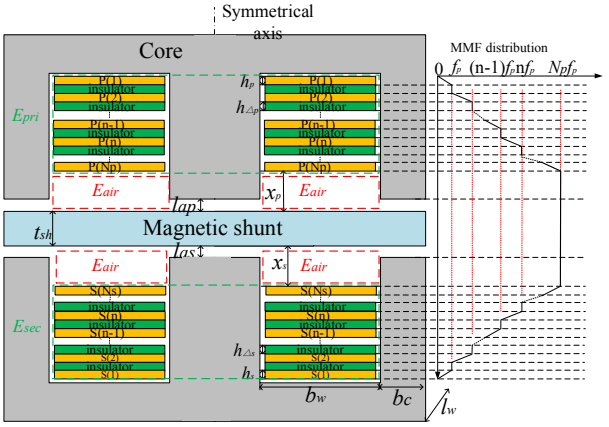

Fig.2. MMF distribution for the shunt-inserted planar transformer with air gaps and both primary and secondary windings away from the shunt

The MMF in the window area is assumed to be N_pf_p. The filed intensity in the air is

$$H_{air}=\frac{N_pf_p}{b_w} \tag{2}$$

Then the energy stored in the air is

$$E_{air}=\frac{1}{2}\mu_0 w_c b_w\int H^2dx \tag{3}$$

Apply (2) into (3), the energy stored in the air is

$$E_{air}=2\cdot\frac{1}{2}\mu_0 w_c\frac{N_p^{\,2}k_p^{\,2}I_p^{\,2}}{b_w}(x_p+x_s) \tag{4}$$

where x_p and x_s are the distance from the primary winding and secondary winding to the shunt, respectively.

The literature [8] gives the energy in the primary and secondary windings, which are

$$E_{pri}=\frac{1}{6}\mu_0\frac{l_w}{b_w}k_p^{\,2}\begin{bmatrix}h_{\Delta p}\left(2N_p^{\,3}-3N_p^{\,2}+N_p\right)\\+2h_pN_p^{\,3}\end{bmatrix}I_p^{\,2} \tag{5}$$

$$E_{\sec}=\frac{1}{6}\mu_0\frac{l_w}{b_w}k_s^{\,2}\begin{bmatrix}h_{\Delta s}\left(2N_s^{\,3}-3N_s^{\,2}+N_s\right)\\+2h_sN_s^{\,3}\end{bmatrix}I_s^{\,2} \tag{6}$$

A. Leakage Inductance due to Magnetic Shunt

The reluctance model is utilized to obtain the leakage inductance created by the magnetic shunt.

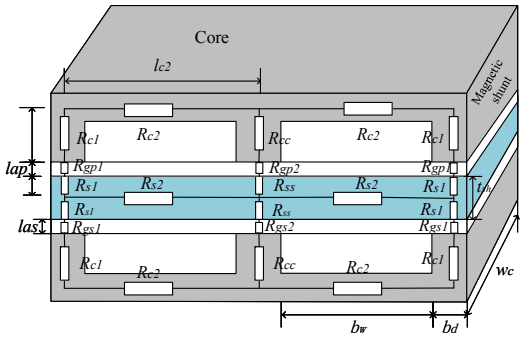

Fig.3. Magnetic reluctance of the planar transformer with magnetic shunt and air gap on three legs

Fig.3 shows the structure of the planar transformer. The air gap is created in each leg by adding an insulation layer. The reluctance of the magnetic core R_{c1}, R_{c2}, R_{cc}, the reluctance of the shunt R_{s1}, R_{s2}, R_{ss} and the reluctance of the air gap R_{gp1}, R_{gp2}, R_{gs1}, R_{gs2} indicated in Fig.3 are given by

$$R_{c1}=\frac{l_{c1}}{\mu_0\mu_r b_d w_c},\quad R_{c2}=\frac{l_{c2}}{\mu_0\mu_r b_d w_c},\quad R_{cc}=\frac{l_{c1}}{\mu_0\mu_r A_c}$$

$$R_{s1}=\frac{t_{sh}}{2\mu_0\mu_s b_d w_c},\quad R_{s2}=\frac{b_w}{\mu_0\mu_s t_{sh} w_c},\quad R_{ss}=\frac{t_{sh}}{2\mu_0\mu_s A_c}$$

$$\begin{aligned}R_{gp1}&=\frac{l_{ap}}{\mu_0(b_d+l_{ap})(w_c+l_{ap})}\\R_{gp2}&=\frac{l_{as}}{\mu_0(2b_d+l_{as})(w_c+l_{as})}\\R_{gs1}&=\frac{l_{as}}{\mu_0(b_d+l_{as})(w_c+l_{as})}\\R_{gs2}&=\frac{l_{as}}{\mu_0(2b_d+l_{as})(w_c+l_{as})}\end{aligned} \tag{7}$$

where μ_0 is the permeability of the air; μ_r and μ_s are the relative permeability of the core and shunt, respectively. A_c is the effective cross-sectional area of the core. Other quantities can be found in Fig.3 Considering the fringing effect, the literature [13] points out a cross section with dimensions a by b would become $(a+g)$ by $(b+g)$. g is the length of the air gap. This is shown in the expression of R_{gp1}, R_{gp2}, R_{gs1}, R_{gs2}.

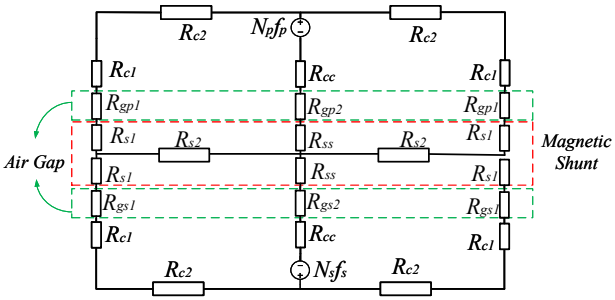

Fig.4. Magnetic reluctance model of the shunt-inserted planar transformer with air gaps

The expression for the inductance calculation based on the equivalent reluctance model shown in Fig.4 is very bulky, but when the air gap length l_{ap} is the same with l_{as},

$$l_{ap} = l_{as} = l_a \tag{8}$$

It leads to

$$R_{gp1} = R_{gs1} = R_{g1}, \quad R_{gp2} = R_{gs2} = R_{g2} \tag{9}$$

Define R_m as

$$R_m = R_{c1} + R_{c2} + 2R_{cc} + R_{s1} + 2R_{ss} \tag{10}$$

The leakage inductance referred to the primary side is

$$L_{k\_shunt} = \frac{4k_p{}^2 N_p{}^2}{R_m + R_{g1} + 2R_{g2} + 2R_{s2}} \tag{11}$$

Combining (1), (4), (5), (6) and (11), the leakage inductance referred to the primary side for the shunt-inserted transformer with air gaps and with both primary and secondary windings away from the shunt is

$$L_k = 2\mu_0 w_c \frac{N_p{}^2 k_p{}^2}{b_w}(x_p + x_s) + \frac{4n_p{}^2}{R_m + R_{g1} + 2R_{g2} + 2R_{s2}} + \frac{1}{3}\mu_0 \frac{l_w}{b_w} k_p{}^2 \sum_{i=p,s}\left[2h_i N_i{}^3 + h_{\Delta i}\left(2N_i{}^3 - 3N_i{}^2 + N_i\right)\right] \tag{12}$$

B. *Verification for the Proposed Calculation Method*

TABLE I. PARAMETERS OF THE TRANSOFORMER

Parameters	Transformer *T1*
Turns per layer in primary k_p	2
Primary layers N_p	4
Primary conductor thickness h_p(mm)	0.07
Insulation thickness in primary $h_{\Delta p}$(mm)	0.2
Turns per layer in secondary k_s	1
Secondary layers N_s	2
Secondary conductor thickness h_s(mm)	0.07
Insulation thickness in secondary $h_{\Delta s}$(mm)	0.2
Shunt thickness t_{sh}(mm)	0.2
Air gap length $2l_a$(mm)	0.2

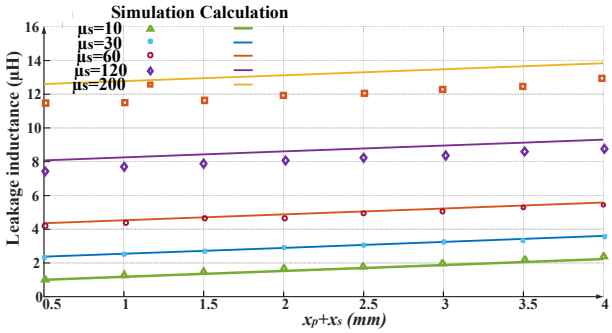

Fig.5. Comparison of leakage inductance obtained by FEA simulations and the proposed calculation method

To verify equation (12), simulations by using 2-D Finite Element Analysis (FEA) are carried out. Details of planar transformers parameters can be found in TABLE I. Fig.5 shows the comparison between the calculation and simulation of leakage inductance for the shunt-inserted planar transformer with different relative permeability of the shunt : 1)μ_s=10;2) μ_s=30;3) μ_s=60;4) μ_s=120;5) μ_s=200. Both the air gap length and shunt thickness are constant. The comparison between the proposed calculation method and FEA simulation for leakage inductance of the proposed planar transformer is shown in Fig.5. The calculation method for the shunt-inserted planar transformer represents good agreement with the FEA simulation.

Three experiment tests were performed by using Agilent 4294A at 1MHz to further prove the calculation. The thickness, relative permeability of the magnetic shunt, the distance from the primary winding and secondary winding to the shunt and air gap length are changed and documented in TABLE II while other parameters are the same with TABLE I. Secondary windings were short circuited when measuring the leakage inductance. Three figures were saved and can be found in the Appendix. The comparison between calculation and experiment tests is shown in Fig.6. It can be seen from test 1 and test 2 that the distance from the primary winding and secondary winding to the shunt can create additional leakage inductance. This proves previous calculation method that the leakage energy in the window area must be considered. Comparing test 2 to test 3, the shunt thickness can also affect the leakage inductance.

In high frequency (above 1MHz) LLC resonant converter design, the resonant inductance is not very large. Thus the magnetic shunt with smaller relative permeability is more preferable. Besides, to achieve lower AC resistance, both primary and secondary windings should be located away from the air gap.

TABLE II. PARAMETERS OF THREE TESTS

Parameters	Three tests		
	Test 1	*Test 2*	*Test 3*
x_p(mm)	2	0	0
x_s(mm)	2	0	0
t_{sh} (mm)	0.15	0.15	0.3
$2l_a$ (mm)	0.1	0.1	0.1
μ_s	45	45	45

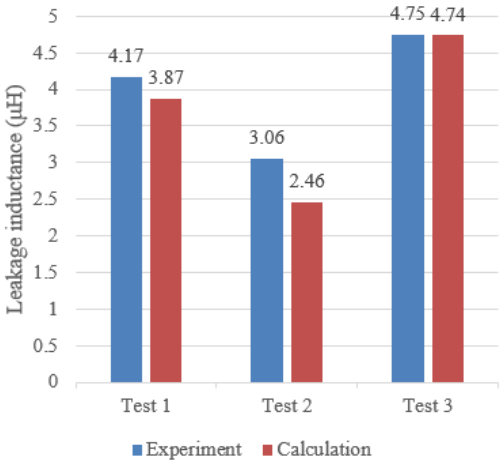

Fig.6. Experimental and calculation results comparison

III. Circuit Parameters Design Cosiderations for LLC

The design of LLC resonant converter is always about the resonant tank design. The resonant tank in LLC converter includes the resonant capacitor C_r, resonant inductor L_r and the magnetizing inductance L_m. In this design, the resonant inductor L_r is integrated into the shunt-inserted planar transformer, which is shown in Fig.7. These three quantities will be specified in the section based on the loss model and desirable switching frequency range.

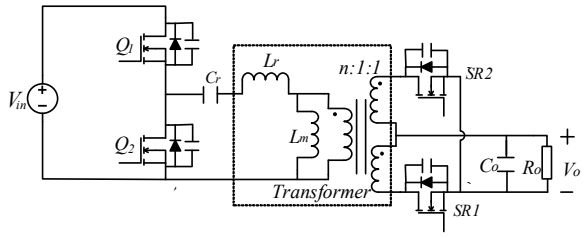

Fig.7. Topology of half bridge LLC resonant converter

A. Conduction and Switching Losses on Semi-conductors

The magnetizing inductance is always related to the both primary and secondary RMS current. In other words, it is well connected with the power loss of LLC converter. The optimal magnetizing inductance can be designed from the analysis of power loss. Primary and secondary RMS current are given in [11].

$$I_{RMS\_pri}=\frac{1}{4\sqrt{2}}\frac{V_o}{nR_L}\sqrt{\frac{n^4{R_L}^2{T_s}^2}{{L_m}^2}+4\pi^2+\frac{16\pi^2\left(T_s t_d+{t_d}^2\right)}{{T_s}^2}} \tag{13}$$

$$I_{RMS\_sec}=\frac{\sqrt{3}}{24\pi}\frac{V_o}{R_L}\sqrt{\frac{\left(5\pi^2-48\right)n^4{R_L}^2{T_s}^3}{{L_m}^2\left(T_s+2t_d\right)}+\frac{12\pi^4 T_s}{T_s+2t_d}+\frac{48\pi^4\left(T_s t_d+{t_d}^2\right)}{T_s\left(T_s+2t_d\right)}} \tag{14}$$

where V_o is the output voltage; n is the transformer turns ratio; R_L is the load resistance; t_d is the dead time; T_s is the switching cycle at resonant frequency. From these two equations, the conduction loss for primary and secondary devices is described as follows:

$$P_{p\_c}=2{I_{pri\_RMS}}^2 R_{p\_DS(\text{on})} \tag{15}$$

$$P_{s\_c}=2{I_{\text{sec}\_RMS}}^2 R_{s\_DS(\text{on})} \tag{16}$$

where $R_{p\_DS(on)}$ and $R_{s\_DS(on)}$ are the drain-to-source resistance of primary devices and secondary devices. Note that (16) is only applicable when synchronous rectification is applied to secondary devices.

Since LLC can achieve ZVS turn-on, only turn-off loss P_{off} exists in primary devices switching loss and is presented by[11]

$$P_{off}=\frac{V_{in}}{3}\left(\frac{V_o}{4nL_m f_{sL}}-C_{pri\_oss}\frac{V_{in}}{T_{off}}\right)T_{off}f_{sw} \tag{17}$$

where T_{off} is the turn-off time; C_{pri_oss} is the output capacitance of primary devices.

B. Transformer Losses Ananlysis

Planar transformer is always applied in high frequency converters due to its very low profile and excellent thermal characteristics. Details about planar transformer design considerations can be found in [15]. Transformer losses consist of core loss and winding loss. The peak flux density is given by

$$B_p=\frac{nV_o\left(T_s/2-T_d\right)}{2N_P A_e} \tag{18}$$

Considering hysteresis loss and eddy current loss, the core loss is calculated by $P_{core}=P_v V_e$, where V_e is the volume of the core and P_v is calculated by Steinmetz's equation: $P_v=K_c f^{\alpha}B_p^{\beta}$. These three quantities K_c,α and β can be calculated from relationship curve between unit volume core loss and flux density given in datasheet. Thus core loss can be represented by

$$P_{core}=K_c f^{\alpha}\left(\frac{nV_o\left(T_s/2-T_d\right)}{2N_P A_e}\right)^{\beta}V_e \tag{19}$$

Dowell's model is the common method for AC winding loss calculation, but its accuracy is affected by the large magnetizing current and the fringing effect brought by flux around air gap. The accurate winding loss can be estimated from 2-D FEA simulations [15].

C. Driving Losses Ananlysis

When the converter operating at high frequency, the driving losses cannot be neglected. It contains the losses for primary switches and secondary synchronous rectifiers and the calculation for them is

$$P_{dr}=2Q_{gs}V_{gs}f_s+2Q_{gs\_sr}V_{gs\_sr}f_s \tag{20}$$

where V_{gs} and V_{gs_sr}, Q_{gs} and Q_{gs_sr} represent the driving voltage and gate-source charge for primary and secondary devices, respectively.

Therefore, the total power loss of the half bridge LLC resonant converter is

$$P_{total} = P_{p\_c} + P_{s\_c} + P_{off} + P_{core} + P_{winding} + P_{dr} \quad (21)$$

It can be concluded that the magnetizing inductance should be maximized to reduce power loss. Meanwhile, as the magnetizing current should discharge all parasitic capacitances during the dead time, magnetizing inductance needs to be smaller enough to allow sufficient magnetizing current to discharge all parasitic capacitances. Thus the magnetizing inductance should be designed to be the largest value that guarantees ZVS. According to [12],

$$L_m = \frac{t_d\left((T_s/2) - t_d\right)}{4\left(2C_{pri\_oss} + 2C_{sec\_oss}\left(\frac{1}{n^2}\right) + C_w\right)} \quad (22)$$

where C_{sec_oss} is the secondary device charge equivalent output capacitance, C_w is the transformer winding capacitance referred to the primary side.

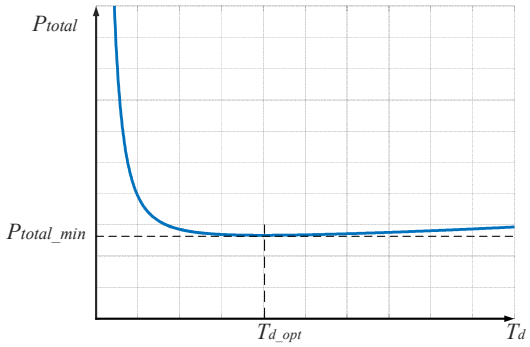

Fig.8. Total power loss as a function of dead time

The equation (22) gives the optimal magnetizing inductance expressed by the dead time. To determine the optimal magnetizing inductance, the total power loss as a function of the dead time, is shown in Fig.8. The optimal T_d can be selected in according with the minimum loss point and then L_m can be determined by the equation (22) with the selected dead time.

D. Inductance Ratio Selection

Based on fundamental harmonic analysis (FHA), resonant frequency, quality factor and inductance ratio should be considered

$$f_r = \frac{1}{2\pi\sqrt{L_r C_r}} \quad (23)$$

$$Q = \frac{\sqrt{L_r/C_r}}{n^2 R_e}, \quad where \quad R_e = \frac{8n^2 R}{\pi^2} \quad (24)$$

$$L_n = \frac{L_m}{L_r} \quad (25)$$

Since this design maintains the resonant frequency constant, the resonant capacitor is determined by the resonant inductor. From previous design, the magnetizing inductance is obtained. Therefore, the real quality factor varies with L_n is expressed in (26) by combining (23), (24) and (25).

$$Q_{real} = \frac{L_m}{L_n}\frac{2\pi f_r}{R_e} \quad (26)$$

The maximum quality factor Q_{max} which allows the required maximum voltage gain at the boundary between capacitive and inductive mode is

$$Q_{\max} = \frac{1}{L_n M_{\max}}\sqrt{L_n + \frac{M_{\max}^2}{M_{\max}^2 - 1}} \quad (27)$$

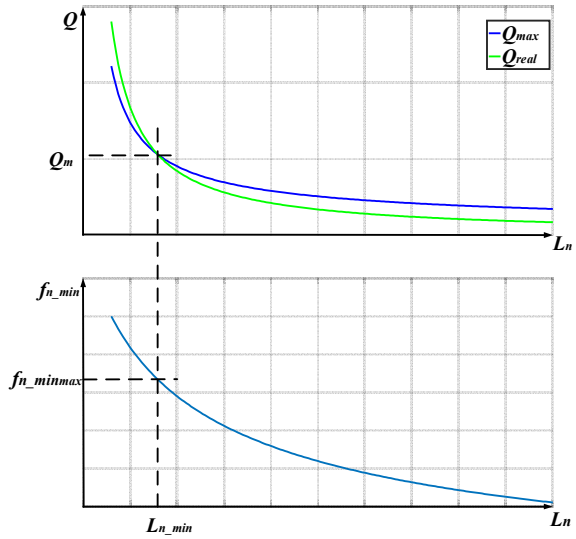

Fig.9. Quality factor and minimum operating frequency as a function of inductance ratio

Considering the given specification, the maximum voltage gain M_{max} is specified. Thus the maximum quality factor is only varied with L_n. This is also seen in minimum operating frequency that allows the converter to achieve the maximum voltage gain, which is expressed by

$$f_{n\_\min} = \sqrt{\frac{1}{1 + L_n\left(1 - \frac{1}{M_{\max}^2}\right)}} \quad (28)$$

Based on (26), (27) and (28), the maximum, real quality factor and minimum operating frequency as a function of the inductance ratio are shown in Fig.9. The real quality factor must be always below the maximum quality factor. The inductance ratio selection should be always larger than L_{n_min}, which allow the quality factor to be smaller than Q_m. Nevertheless, larger L_n means the switching frequency range is wider. The regulation capability of the converter becomes weaker. Therefore, the inductance ratio should be designed carefully to achieve ZVS in whole load range and obtain narrowed switching frequency.

IV. Experimental Implementation

A 1 MHz, 100W half bridge LLC resonant converter is built, as shown in Fig.10. Detailed Circuit specifications and the proposed planar transformer parameters are listed in TABLE III and TABLE IV, respectively. In this design, the resonant inductor is integrated into the planar transformer by using its leakage inductance created by the magnetic shunt. The selected inductance ratio was 7.2 to narrow the switching frequency. The core used in this converter was E32/6/20-3F46 and the 8:2:2 turns ratio was conducted to

achieve desirable magnetizing and leakage inductance. GS66508T from GaN system is selected for primary devices due to its low effective output capacitance and on-state resistance compared with Silicon devices.

The waveform of the converter operating at resonant frequency (1 MHz) with 380V input and 48V output is shown in Fig.11 (a). To achieve GaN devices safe operation, the output gate signal from gate driver has negative voltage. It can be seen that ZVS turn-on is achieved because the drain-to-source voltage drops right down to zero when the gate becomes high. Thus the reverse conduction through GaN devices is greatly minimized. Fig.11 (b) shows the waveforms of the converter operating at 700 kHz with 280V input and 48V-100W output. ZVS operation is also achieved.

TABLE III. CIRCUIT SPECIFICATIONS AND PARAMETERS

Parameters	Values
Input voltage	280-380V
Output voltage V_o	48V
Output power P_o	100W
Magnetizing inductance L_m	31μH
Resonant inductance L_r	4.3μH
Resonant capacitance C_r	5.59nF
Turns-ratio n	8:2:2
Primary devices	GS66508T
Secondary devices	FSV15120V
Core type and material	E32/6/20-3F46

TABLE IV. PARAMETERS OF THE DESIGNED TRANSOFORMER

Parameters	Transformer
Turns per layer in primary k_p	2
Primary layers N_p	4
Primary conductor thickness h_p(mm)	0.07
Insulation thickness in primary $h_{\Delta p}$(mm)	0.25
Turns per layer in secondary k_s	1
Secondary layers N_s	4
Secondary conductor thickness h_s(mm)	0.07
Insulation thickness in secondary $h_{\Delta s}$(mm)	0.25
Shunt thickness t_{sh}(mm)	0.15
Air gap length $2l_a$(mm)	0.2
Permeability of magnetic shunt μ_s	45
Distance between primary windings and the shunt x_p (mm)	2
Distance between primary windings and the shunt x_s (mm)	2

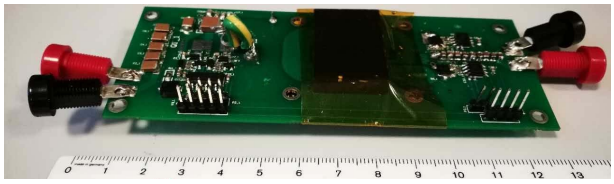

Fig.10. Prototype of 1MHz 100W LLC resonant converter

Due to the small inductance ratio, switching frequency range is greatly narrowed. Switching frequency swings from 700 kHz to 1MHz to accommodate input voltage changing from 280V to 380V. To further prove the proposed transformer with increased leakage inductance can narrow the switching frequency, the half bridge LLC resonant converter operating at 150V input and 48V-100W output is investigated as shown in Fig.11 (c). Switching frequency under this case now becomes 500 kHz. Therefore, this transformer structure is well adapted to LLC resonant converter to be capable to handle wide input voltage range within narrowed switching frequency.

The loss breakdown for the total system at 1MHz with 380V input and 48V-100W output is shown in Fig.12. The main power loss comes from the winding loss and secondary diodes conduction loss, which can be reduced by applying synchronous rectifiers. Efficiency curves of the converter under different input voltages and load conditions are illustrated in Fig.13. When input voltage drops, the corresponding switching frequency also decreases to maintain constant output voltage. Thus the transformer AC resistance is reduced. The switching frequency deviates from the resonant frequency causing additional circulation energy loss, but the decreased winding loss may improve total system efficiency at light load especially in high frequency applications. With the increasing output power, both circulation power loss and winding loss become larger due to the larger primary current. Thus the total system efficiency drops.

The built prototype with the proposed transformer structure and diode rectifiers can still achieve more than 90% peak efficiency. Moreover, the total system efficiency can be improved by using synchronous rectifiers.

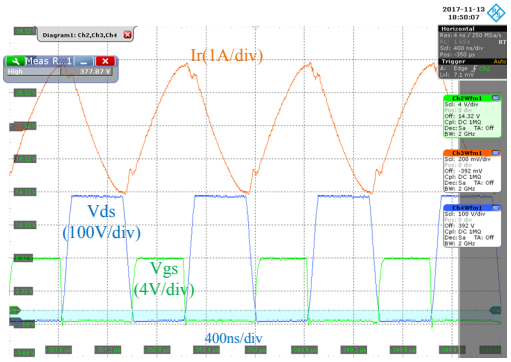

(a)

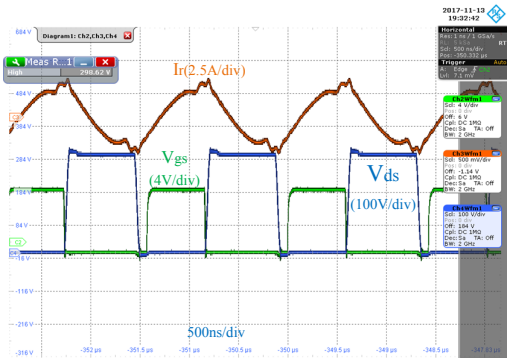

(b)

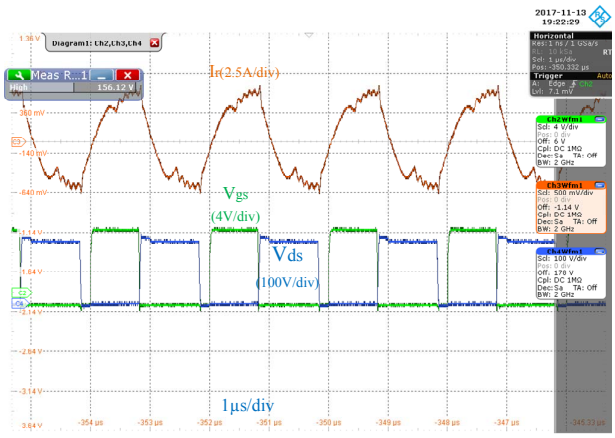

(c)

Fig.11. 100W LLC resonant converter operating at (a) 1MHz with 380V input (b) 700kHz with 280V input (c) 500kHz with 150V input and 48V-100W output

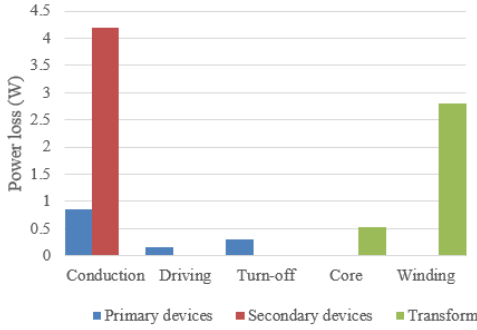

Fig.12. Loss breakdown for the converter operating at 1MHz with 380V input and 48V-100W output

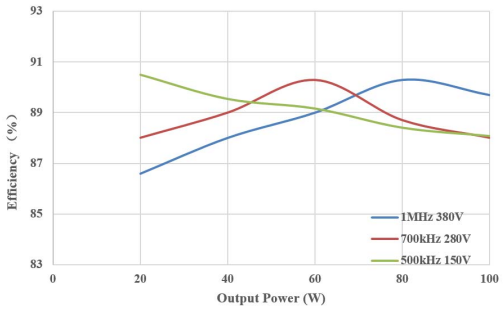

Fig.13. Efficiency of LLC converter at different load conditions

V. Conclusion

In this paper, a planar transformer structure with a magnetic shunt and air gaps is proposed to create large leakage inductance. The leakage inductance calculation methodology is verified by 2-D FEA simulations and experiment tests. The built prototype proves that the transformer structure is well adapted to the LLC resonant converter to integrate resonant inductor into transformer. Moreover, instead of increasing regulation capability by decreasing magnetizing inductance which increases the total system power loss, the proposed transformer structure and design methodology maintain the optimal magnetizing inductance while increase leakage inductance to obtain the narrowed switching frequency with wide input voltage range.

As a result, a high efficiency half bridge LLC resonant converter operating at 1MHz 100W with wide input voltage range and narrowed switching frequency is built with the proposed planar transformer. Due to the small inductance ratio, high regulation capability is achieved. Since there is no additional winding and magnetic core, the power density can be improved.

Appendix

In this appendix, it shows the leakage inductance curves captured by Agilent 4294A are shown in Fig.14 (a) to (c).

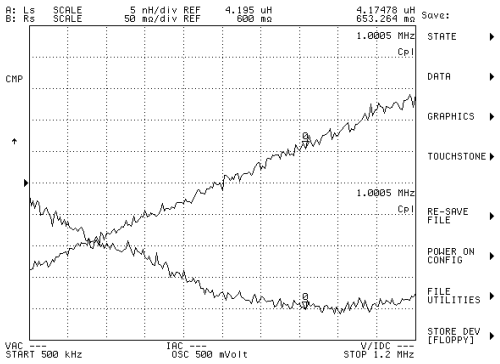

(a)

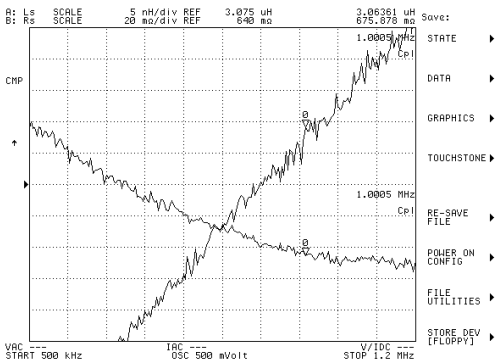

(b)

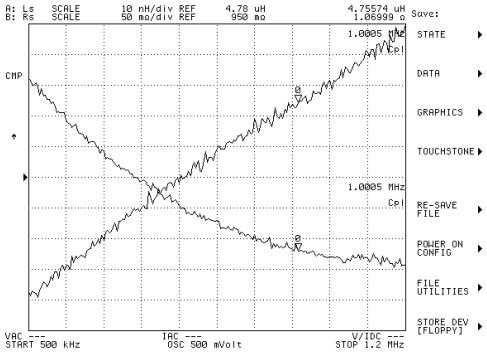

(c)

Fig.14. Leakage inductance for (a) test 1 (b) test 2 (c) test 3

REFERENCES

[1] C. Fei, F. C. Lee, and Q. Li, "High-efficiency High-power-density LLC Cocnverter with an Integrated Planar Matrix Transformer for High Output Current Applications," *IEEE Transactions on Industrial Electronics*, pp. 1–1, 2017.

[2] B. Yang and F. C. Lee, "LLC Resonant Converter for Front End DC / DC Conversion," *Applied Power Electronics Conference and Exposition*, vol. 2,pp. 1108–1112, 2002

[3] Z. Fang, T. Cai, S. Duan, and C. Chen, "Optimal Design Methodology for LLCResonant Converter in Battery Charging Applications Based on Time-Weighted Average Efficiency," *IEEE Transactions on Power Electronics*, vol. 30, no. 10, pp. 5469–5483, 2015.

[4] Y.-C. Li, F. C. Lee, Q. Li, X. Huang, and Z. Liu, "A novel AC-to-DC adaptor with ultra-high power density and efficiency," *2016 IEEE Applied Power Electronics Conference and Exposition (APEC)*, 2016.

[5] Y. Jeong, G.-W. Moon, and J.-K. Kim, "Analysis on half-bridge LLC resonant converter by using variable inductance for high efficiency and power density server power supply," *2017 IEEE Applied Power Electronics Conference and Exposition (APEC)*, 2017.

[6] Y. Chen, H. Wang, Z. Hu, Y.-F. Liu, J. Afsharian, and Z. A. Yang, "LCLC resonant converter for hold up mode operation," *2015 IEEE Energy Conversion Congress and Exposition (ECCE)*, 2015. M. Cui, X. You, Y. Li, and M. Liang, "Planar transformer design in GaN based LLC resonant converter," *2014 International Power Electronics and Application Conference and Exposition*, 2014.

[7] K. Tan, R. Yu, S. Guo, and A. Q. Huang, "Optimal design methodology of bidirectional LLC resonant DC/DC converter for solid state transformer application," *IECON 2014 - 40th Annual Conference of the IEEE Industrial Electronics Society*, 2014.

[8] J. Zhang, Z. Ouyang, M. C. Duffy, M. A. E. Andersen, and W. G. Hurley, "Leakage inductance calculation for planar transformers with a magnetic shunt," *IEEE Transactions on Power Electronics*, vol. 50, no. 6, pp.4107-4112. 2014.

[9] M.-X. Li, Z. Ouyang, B. Zhao, M.A. E. Andersen，"Analysis and Modeling of Integrated Magnetics for LLC resonant Converters" *IECON 2017- 43h Annual Conference of the IEEE Industrial Electronics Society*, 2017

[10] Z. Ouyang, J. Zhang, and W. G. Hurley, "Calculation of Leakage Inductance for High-Frequency Transformers," *IEEE Transactions on Power Electronics*, vol. 30, no. 10, pp. 5769–5775, 2015.

[11] J.-Y. Lee, Y.-S. Jeong, and B.-M. Han, "An Isolated DC/DC Converter Using High-Frequency Unregulated LLC Resonant Converter for Fuel Cell Applications," *IEEE Transactions on Industrial Electronics*, vol. 58, no. 7, pp. 2926–2934, 2011.

[12] W. Zhang, F. Wang, D. J. Costinett, L. M. Tolbert and B. J. Blalock,"Investigation of Gallium Nitride Devices in High-Frequency LLC Resonant Converters," *IEEE Transactions on Power Electronics*, vol.32, no. 1, pp. 571-583, Jan. 2017.

[13] W. G. Hurley and W. H. Wölfle, "Transformers and Inductors for Power Electronics," Aug. 2013.

[14] Z. Ouyang and Michael A. E. Andersen. "Overview of Planar Magnetic Technology—Fundamental Properties." *IEEE Transactions on Power Electronics*, vol. 29, no. 9, 2014, pp. 4888–4900.

[15] B. Li, Q. Li, and F. C. Lee, "A novel PCB winding transformer with controllable leakage integration for a 6.6kW 500kHz high efficiency high density bi-directional on-board charger," *IEEE Applied Power Electronics Conference and Exposition (APEC)*, 2017.